Spin gap in the normal state of Pr-doped and oxygen-deficient RBa$_2$Cu$_3$O$_7$ superconductors

S. J. Liu* and Weiyan Guan

Materials Science Center and Department of Physics, National Tsing Hua University, Hsinchu, Taiwan, Republic of China

(Received 10 November 1997; revised manuscript received 17 March 1998)

The spin-gap temperatures (T_S) in the normal state of bulk Pr-doped RBa$_2$Cu$_3$O$_7$ (R_{1-x}Pr$_x$Ba$_2$Cu$_3$O$_7$) and oxygen-deficient RBa$_2$Cu$_3$O$_x$ (R=Yb, Er, Y, Ho, Dy, Gd, Eu, Sm, and Nd) are investigated. The elements on the R sites and the distance between CuO$_2$ planes are found to have no influence on T_S in oxygen-deficient RBa$_2$Cu$_3$O$_x$ in terms of the relationship between the superconducting temperature (T_C) and T_S. However, for R_{1-x}Pr$_x$Ba$_2$Cu$_3$O$_7$, T_S increases with increasing ionic size of R-site elements for a fixed Pr concentration. Furthermore, by comparing T_S of oxygen-deficient RBa$_2$Cu$_3$O$_x$ to that of R_{1-x}Pr$_x$Ba$_2$Cu$_3$O$_7$ at the same T_C, it is observed that Pr atoms doped on the R sites not only reduce the carrier density and induce the spin gap, but will also simultaneously suppress T_S. [S0163-1829(98)05837-8]

I. INTRODUCTION

The in-plane resistivity $R_{ab}(T)$ of an optimally doped RBa$_2$Cu$_3$O$_7$ superconductor is linear with respect to temperature in the normal state. However, $R_{ab}(T)$ apparently deviates from the T-linear behavior below T_S, the temperature at which a spin gap opens, well above T_C, for the underdoped YBa$_2$Cu$_3$O$_7$ (Refs. 1 and 2) and YBa$_2$Cu$_4$O$_8$.[3] This phenomenon indicates a suppression of carrier scattering at low temperature. Moreover, T_S increases with reduction of the doping level of an underdoped YBa$_2$Cu$_3$O$_7$. However, the spin gap does not seem to be a true energy gap and has been referred to as a ''pseudogap'' or ''spin pseudogap.'' The details of the crossover at T_S are not clear at the moment. The crossover temperature T_S may be associated with the development of an antiferromagnetic correlation.

The problem of the oxygen deficiency in the YBa$_2$Cu$_3$O$_7$ system was studied widely.[4] The reduction of carrier density is one of the main effects resulting from the oxygen deficiency. O atoms in CuO chains are removed when the oxygen content is reduced and the carrier numbers in CuO$_2$ planes decrease by virtue of the reduction of holes transferred from CuO chains to CuO$_2$ planes. Consequently, an oxygen-deficient YBa$_2$Cu$_3$O$_x$ is underdoped and T_C is suppressed.

Among the rare earth element-substituted isomorphic YBa$_2$Cu$_3$O$_7$ superconductors, PrBa$_2$Cu$_3$O$_7$ is an exception which fails to exhibit superconductivity.[5] The suppression of the superconductivity of the Y$_{1-x}$Pr$_x$Ba$_2$Cu$_3$O$_7$ system is strongly related to the Pr concentration[6,7] and attributed to three possible mechanisms. The first mechanism is the filling or localization of mobile holes in the conducting CuO$_2$ planes, which assumes a 4+ or mixed valence state for Pr. The process by which additional valence electrons fill the holes in CuO$_2$ planes reduces the number of carriers and inhibits superconductivity. The second mechanism is the pair-breaking effect with Pr^{3+} acting as a strong pair-breaker. The relation between T_C and Pr concentration can be well-fitted by the Abrikosov-Gor'kov (AG) pair-breaking theory.[8] The third mechanism is a refined model combining features of hole filling/localization and pair-breaking. This model is based on a strong hybridization between the Pr 4f and O 2p orbits in the CuO$_2$ planes.[9,10] The magnetic interactions and localization effects resulting from hybridization can cause a larger hopping barrier and localize the holes.

An ion-size effect was observed in the experiments on the R_{1-x}Pr$_x$Ba$_2$Cu$_3$O$_7$ system (R=Nd, Eu, Gd, Y, Er, and Yb).[11] The results of these investigations indicate that T_C decreases monotonically with increasing Pr concentration. In addition, T_C decreases approximately linearly with increasing radius of the R-site ions for a fixed dopant amount x. Guan *et al.* demonstrated that the antiferromagnetic ordering temperature (T_N) of the Pr ions,[12] the normal state resistivity, and the Hall number of $R_{0.8}$Pr$_{0.2}$Ba$_2$Cu$_3$O$_7$[13] are also ion-size dependent.

The substitution of Pr for Y in YBa$_2$Cu$_3$O$_7$ reduces the doping level and causes the Y$_{1-x}$Pr$_x$Ba$_2$Cu$_3$O$_7$ to be underdoped, as deduced from the hole filling/localization mechanism. For Y$_{1-x}$Pr$_x$Ba$_2$Cu$_3$O$_7$, a deviation from the T-linear resistivity behavior[14] is observed. The $(T_1T)^{-1}$ vs T curve, measured at ^{63}Cu sites in an NMR experiment,[15] shows a peak at T_S, well above T_C. These observations are similar to those made in oxygen-deficient YBa$_2$Cu$_3$O$_x$ samples.

Francois *et al.* studied the effects of Pr doping and oxygen deficiency on the complex conductivity and scattering rate of YBa$_2$Cu$_3$O$_x$ thin films.[16] They concluded that the spin-gap behaviors are completely determined by the carrier density, as indicated by the similarity of the spin-gap temperatures at a fixed T_C in both Pr-doped and oxygen-deficient samples. The similarity between the two types of samples also implies that the only effect of Pr ions is the depletion of mobile carriers in the CuO$_2$ planes. Apparently, the magnetic character of the Pr ions has no influence on superconductivity.

We believe that hybridization between Pr ions and CuO$_2$ planes in PrBa$_2$Cu$_3$O$_7$ and R_{1-x}Pr$_x$Ba$_2$Cu$_3$O$_7$ systems is consistent with the results of many ion-size effect experiments in R_{1-x}Pr$_x$Ba$_2$Cu$_3$O$_7$. Furthermore, we suggest that the hybridization will influence the spin-gap temperature of the R_{1-x}Pr$_x$Ba$_2$Cu$_3$O$_7$ system.

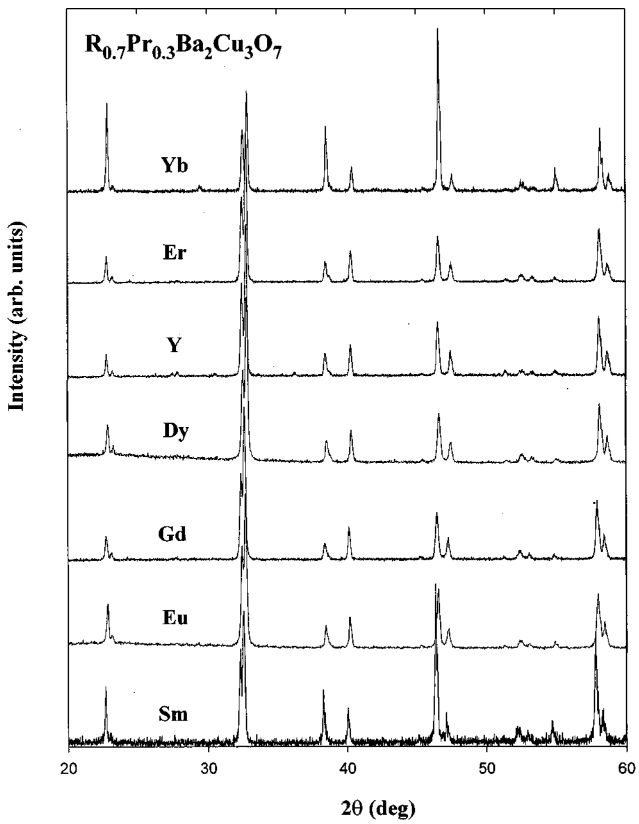

FIG. 1. X-ray diffraction patterns of $R_{0.7}Pr_{0.3}Ba_2Cu_3O_7$ (R = Er, Y, Ho, Dy, Gd, Eu, and Sm) systems.

The resistivity of $R_{1-x}Pr_xBa_2Cu_3O_7$ (R = Yb, Er, Y, Dy, Gd, Eu, Sm, and Nd) and oxygen-deficient $RBa_2Cu_3O_x$ (R = Er, Y, Ho, Dy, Gd, Eu, and Sm) was measured. Subsequently, T_C and T_S were determined from the resistivity curves, in order to investigate the ion-size effect and the influence of hybridization on T_S.

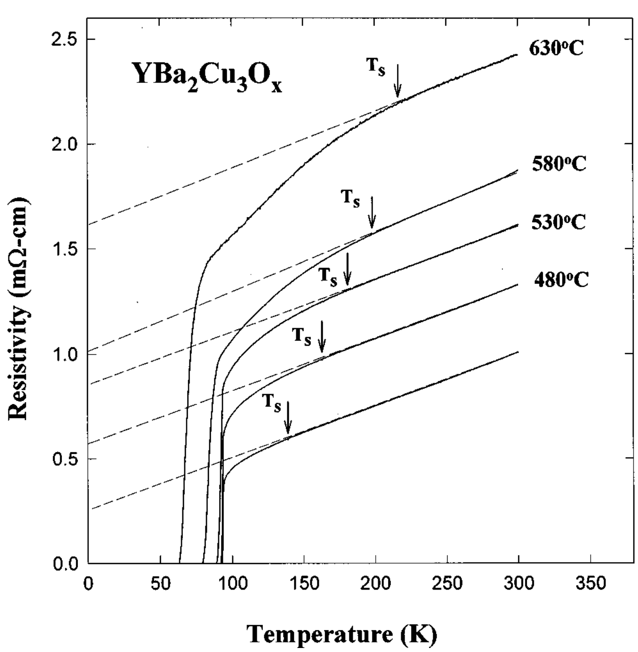

FIG. 2. Electrical resistivity $R(T)$ of oxygen deficient $YBa_2Cu_3O_x$. The temperatures noted beside the curves are the quenching temperatures.

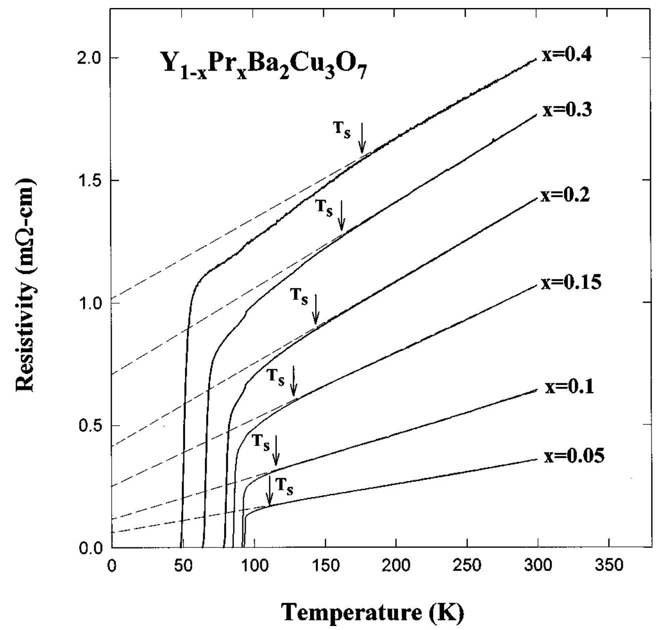

FIG. 3. Electrical resistivity $R(T)$ of $Y_{1-x}Pr_xBa_2Cu_3O_7$.

II. EXPERIMENT

The ceramic samples $R_{1-x}Pr_xBa_2Cu_3O_7$ (R = Yb, Er, Y, Dy, Gd, Eu, Sm, and Nd) and $RBa_2Cu_3O_7$ (R = Er, Dy, Gd, and Sm) were prepared by a standard solid-state reaction method and $RBa_2Cu_3O_7$ (R = Y, Ho, and Eu) by a chemical coprecipitation method.[17] Appropriate mixtures of high purity (99.9%) CuO, $BaCO_3$, Pr_6O_{11}, and R_2O_3 were thoroughly mixed, ground and calcined at 850 °C, 870 °C and 890 °C for 12 h in air, and then slowly cooled in a furnace. The powders were ground carefully before each calcined procedure. Subsequently, the powders were ground again and pressed into pellets at 400 Kg/cm^2. The pellets were then sintered at a fixed temperature between 935 °C and 950 °C for 48 h and annealed at 450 °C for 24 h in flowing oxygen.

The structure and phase purity of all samples were examined using a Rigaku Rotaflex rotating anode powder x-ray diffractometer which uses Cu $K\alpha$ radiation with wavelength $\lambda = 1.5406$ Å. The x-ray diffraction (XRD) patterns show that each sample possesses the layered perovskite-like struc-

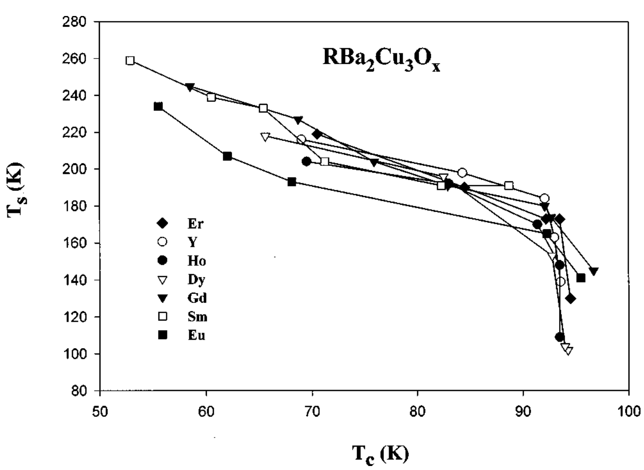

FIG. 4. T_C vs T_S for oxygen-deficient $RBa_2Cu_3O_x$ (R = Er, Y, Ho, Dy, Gd, Sm, and Eu) systems.

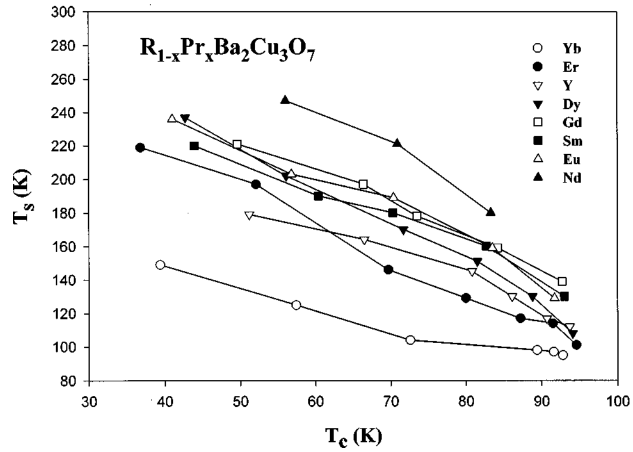

FIG. 5. T_C vs T_S for $R_{1-x}Pr_xBa_2Cu_3O_7$ (R=Yb, Er, Y, Dy, Gd, Sm, Eu, and Nd) systems.

ture and contain no extra peaks, due to impurity phase, within the experimental error. As an example, Fig. 1 displays the XRD patterns of 30%-Pr-doped $RBa_2Cu_3O_7$.

The $RBa_2Cu_3O_x$ samples were heated and kept at a fixed temperature (the quenching temperature, T_Q) between 480 °C and 630 °C in flowing oxygen. The samples were then quenched after 24 h from T_Q to the ambient temperature by pulling them from the furnace into air to reduce their oxygen content. Samples with different oxygen content were obtained by varying T_Q. Higher T_Q corresponds to higher resistivity in the normal state, but lower oxygen content and lower T_C. In order to ensure that the samples were not destroyed by repetitive quenching procedures and resistivity measurements, all samples were fully oxygenated again, and their resistivities measured, after the experimental procedures. The superconductivity and resistivity of all of the samples could be recovered after fully oxygenated, confirming that the samples were not destroyed in the experimental procedures.

The resistivity measurements, from 300 K down to the zero resistivity temperature, were carried out by the standard four-probe method with silver paste or indium contact on regular bars sliced from the sintered sample. Figure 2 and

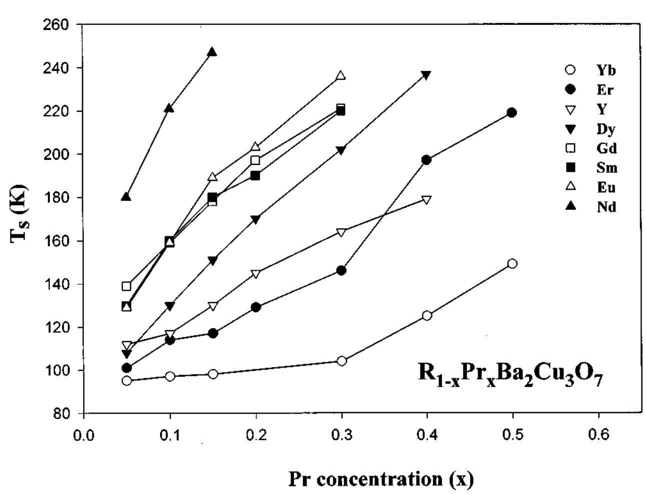

FIG. 6. Pr concentration vs T_S for $R_{1-x}Pr_xBa_2Cu_3O_7$ (R=Yb, Er, Y, Dy, Gd, Sm, Eu, and Nd) systems.

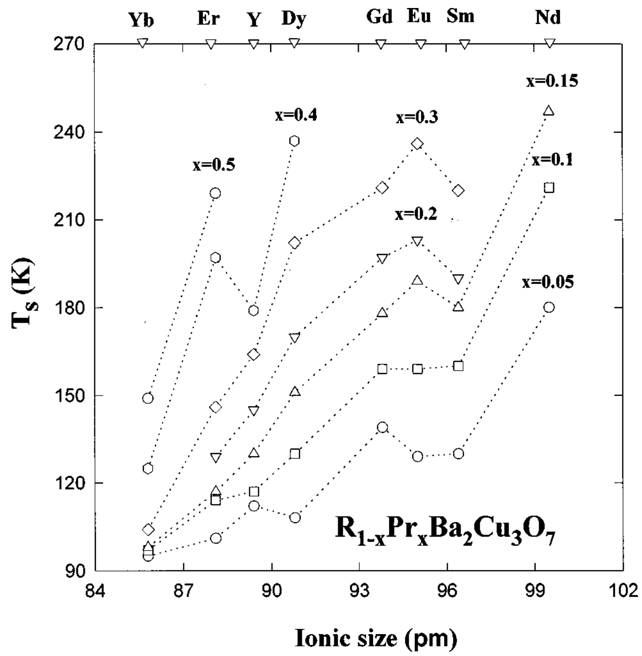

FIG. 7. Ionic size vs T_S of $R_{1-x}Pr_xBa_2Cu_3O_7$ (R=Yb, Er, Y, Dy, Gd, Sm, Eu, and Nd) systems.

Fig. 3 illustrate the resistivity curves of oxygen-deficient $YBa_2Cu_3O_x$ and $Y_{1-x}Pr_xBa_2Cu_3O_7$.

T_C is determined from the midpoint of the superconducting transition width and T_S is defined as the deviation point of the linear resistivity curve.

III. RESULTS AND DISCUSSION

The comparison of the spin-gap temperature of the oxygen-deficient $RBa_2Cu_3O_x$ with that of $R_{1-x}Pr_xBa_2Cu_3O_7$ was made using T_C as a carrier density indicator. This was made possible by the fact that spin-gap behaviors are largely controlled by the carrier density and T_C can serve as an effective carrier density indicator because the trend of T_C vs hole-carrier number curve is the same in the region $T_C > 60$ K for both $Y_{1-x}Pr_xBa_2Cu_3O_7$ and oxygen-deficient $YBa_2Cu_3O_X$.[18]

Figure 4 displays the T_S vs T_C curves of oxygen-deficient $RBa_2Cu_3O_x$. The result shows that all of the samples with different R-site elements have similar T_S vs T_C behaviors, that all T_S are similar at a fixed T_C, and that there is no regularity in T_S due to the ionic size of R-site elements. This result indicates that the rare earth elements on the R sites and the distance between adjacent CuO_2 planes have no influence on the spin-gap temperature.

Unlike the oxygen-deficient $RBa_2Cu_3O_x$, the rare earth elements between the adjacent CuO_2 planes in the $R_{1-x}Pr_xBa_2Cu_3O_7$ do influence the spin-gap temperature because of the Pr substitution. The values of T_S are quite different at a given T_C, though the trends are similar. This is shown in Fig. 5, which displays the relationship between T_C and T_S of $R_{1-x}Pr_xBa_2Cu_3O_7$ with different R-site elements.

T_S as a function of the Pr concentration, presented in Fig. 6, increases almost linearly with increasing Pr concentration. Figure 7 displays the relationship between the ionic size of the R-site elements and T_S in $R_{1-x}Pr_xBa_2Cu_3O_7$. On the

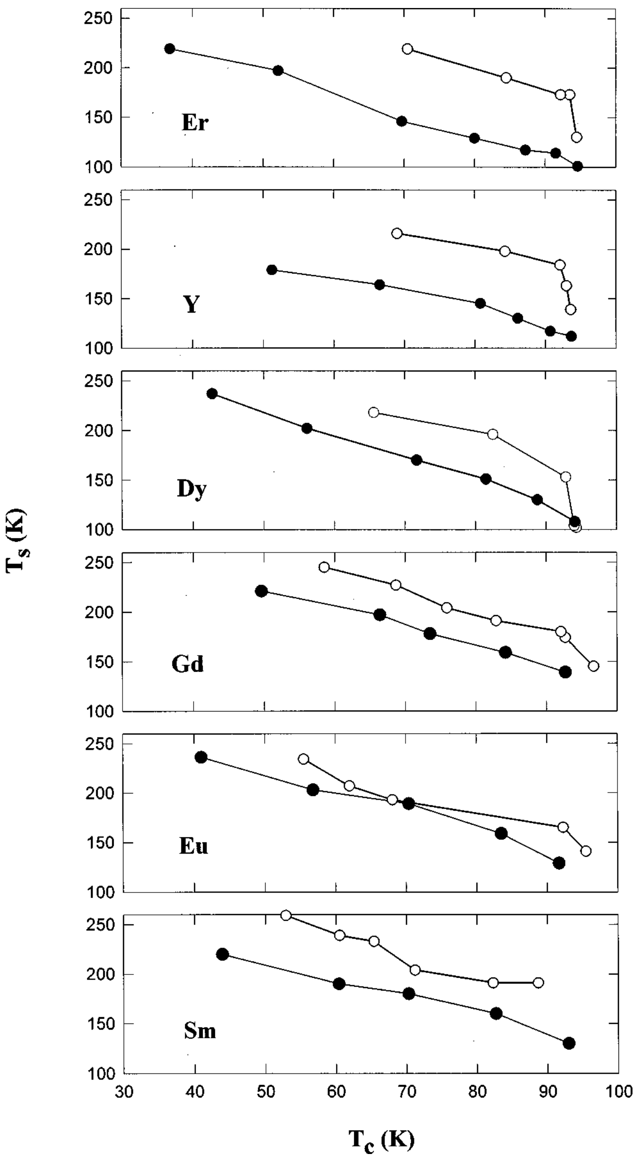

FIG. 8. T_C vs T_S for $R_{1-x}Pr_xBa_2Cu_3O_7$ and oxygen-deficient $RBa_2Cu_3O_x$ (R=Er, Y, Dy, Gd, Eu, and Sm) systems. ○: oxygen-deficient $RBa_2Cu_3O_x$; ●: $R_{1-x}Pr_xBa_2Cu_3O_7$.

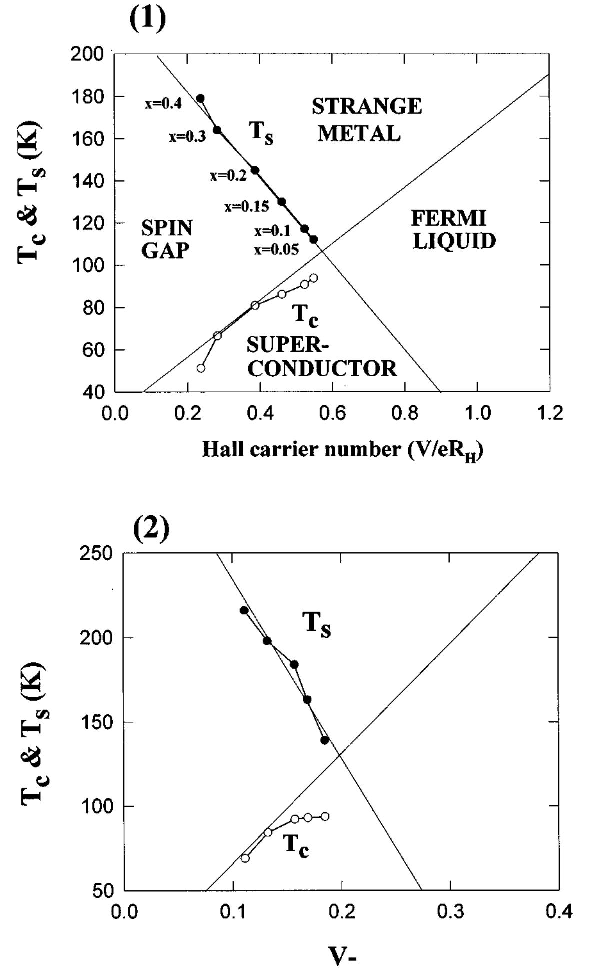

FIG. 9. T_C and T_S vs doping level for (1) $Y_{1-x}Pr_xBa_2Cu_3O_7$ and (2) oxygen-deficient $YBa_2Cu_3O_x$. $V_- = [2 + V_{Cu(2)} - V_{O(2)} - V_{O(3)}]$: the total hole density in the CuO_2 planes.

whole, T_S increases with increasing ionic size for a fixed Pr concentration.

As shown in Fig. 8, which relates T_S of oxygen-deficient $RBa_2Cu_3O_x$ to that of $R_{1-x}Pr_xBa_2Cu_3O_7$, the T_S of Pr-doped samples is much lower than that of oxygen-deficient samples at the same T_C. In addition, the hole-carrier number of a $Y_{1-x}Pr_xBa_2Cu_3O_7$ is just slightly larger than that of an oxygen-deficient $YBa_2Cu_3O_x$ (Ref. 18) at the same T_C in the region $T_C > 60$ K. However, the small difference in the hole-carrier number between $Y_{1-x}Pr_xBa_2Cu_3O_7$ and oxygen-deficient $YBa_2Cu_3O_x$, at the same T_C, should not result in so large a difference in T_S if the spin-gap behaviors are completely determined by the carrier density. The reduction of carrier density, resulting from Pr doping, will induce the spin gap, but the Pr doped between CuO_2 planes will also simultaneously suppress T_S. It may be deduced that the hybridization between Pr and CuO_2 planes will influence the spin-gap temperature since the spin gap occurs in CuO_2 planes. The hybridization in the small R-site ion $R_{1-x}Pr_xBa_2Cu_3O_7$ systems (for example, R=Er or Y) is stronger than that in the large R-site ion $R_{1-x}Pr_xBa_2Cu_3O_7$ systems (for example, R=Eu or Sm), because the distance between the adjacent CuO_2 planes in $R_{1-x}Pr_xBa_2Cu_3O_7$ (R=Er or Y) is shorter than that in $R_{1-x}Pr_xBa_2Cu_3O_7$ (R=Eu or Sm). Thus, the difference in T_S between oxygen-deficient and Pr-doped samples is larger for the smaller ions at the same T_C.

A general mean-field phase diagram, based on Anderson's resonating valence bond (RVB) theory, for the HTSC's as a function of hole doping has been proposed by Nagaosa and Lee.[19] There are two characteristic temperatures related to two phase transitions in the phase diagram. One is the spin-gap temperature T_g (T_S in this work) below which the spinons become paired, and the other is the Bose-Einstein condensation temperature T_{BE} (T_C in the underdoped samples) below which the holons condense. Since the holons, which are responsible for conductivity, are solely scattered by the spinons, the decrease of scattering centers which is due to the pairing of spinons causes resistivity to reduce rapidly below T_S. This explains the deviation from the T-linear behavior, as observed in experiments. In Fig. 9, we present the data of $Y_{1-x}Pr_xBa_2Cu_3O_7$ and oxygen-deficient $YBa_2Cu_3O_x$ in the mean-field phase diagram. The hole content of the $Y_{1-x}Pr_xBa_2Cu_3O_7$ is obtained from the relation between Hall carrier number and T_C in Ref. 20 and the data for the oxygen-deficient $YBa_2Cu_3O_x$ comes from Ref. 21. Our data, for both $Y_{1-x}Pr_xBa_2Cu_3O_7$ and oxygen-deficient $YBa_2Cu_3O_x$, fits well within the mean-field phase diagram.

IV. CONCLUSION

From our study we concluded that the spin gap is not completely determined by the carrier density. It will also be suppressed by the hybridization between Pr $4f$ electrons and CuO_2 planes in the $R_{1-x}Pr_xBa_2Cu_3O_7$ system.

In addition, the *R*-site rare earth elements and the distance between adjacent CuO_2 planes have no influence on the spin gap since the relationships between T_S and T_C of various oxygen-deficient $RBa_2Cu_3O_x$ are similar. However, T_S increases with increasing ionic size of *R*-site elements for a fixed Pr concentration in $R_{1-x}Pr_xBa_2Cu_3O_7$ (R = rare earth element).

ACKNOWLEDGMENTS

We thank Professor C. C. Chi, Professor Y. S. Guo, and Y. C. Liao for helpful discussion, and Dr. S. R. Sheen and J. C. Huang for experimental assistance. This work was supported by the National Science Council of Taiwan, R.O.C.

*Present address: Department of Electrophysics, National Chiao Tung University, Hsinchu, Taiwan, Republic of China.

[1] T. Ito, K. Takenaka, and S. Uchida, Phys. Rev. Lett. **70**, 3995 (1993).
[2] K. Takenaka, K. Mizuhashi, H. Takagi, and S. Uchida, Phys. Rev. B **50**, 6534 (1994).
[3] B. Bucher, P. Steiner, T. Karpinski, E. Kaldis, and P. Wachter, Phys. Rev. Lett. **70**, 2012 (1993).
[4] For example, R. J. Cava, A. W. Hhewat, E. A. Hewat, B. Batlogg, M. Marezio, K. M. Rabe, J. J. Krajewski, W. F. Peck, Jr., and L. W. Rupp, Jr., Physica C **165**, 419 (1990).
[5] H. B. Radousky, J. Mater. Res. **7**, 1917 (1992).
[6] J. K. Liang, X. T. Xu, S. S. Xie, G. H. Rao, X. Y. Shao, and Z. G. Duan, Z. Phys. B **69**, 137 (1987).
[7] Y. Dalichaouch, M. S. Torika Chvili, E. A. Early, B. W. Lee, C. L. Seaman, K. N. Yang, H. Zhou, and M. B. Maple, Solid State Commun. **65**, 1001 (1988).
[8] A. A. Abrikosov and L. P. Gor'kov, Zh. Eksp. Teor. Fiz. **39**, 1781 (1960) [Sov. Phys. JETP **12**, 1243 (1961)]; Yunhui Xu and Weiyan Guan, Appl. Phys. Lett. **59**, 2183 (1991).
[9] J. B. Torrance and R. M. Metzger, Phys. Rev. Lett. **63**, 1515 (1989).
[10] R. Fehrenbacher and T. M. Rice, Phys. Rev. Lett. **70**, 3471 (1993).
[11] Yunhui Xu and Weiyan Guan, Phys. Rev. B **45**, 3176 (1992), and references therein.
[12] Weiyan Guan, Yunhui Xu, S. R. Sheen, Y. C. Chen, J. Y. T. Wei, H. H. F. Lai, and M. K. Wu, Phys. Rev. B **49**, 15 993 (1994).
[13] J. C. Chen, Yunhui Xu, M. K. Wu, and Weiyan Guan, Phys. Rev. B **53**, 5839 (1996).
[14] R. Buhleier, S. D. Broson, I. E. Trofimov, J. O. White, H.-U. Habermeier, and J. Kuhl, Phys. Rev. B **50**, 9672 (1994).
[15] A. P. Reyes, D. E. MacLaughlin, M. Takigawa, P. C. Hammel, R. H. Heffner, J. D. Thompson, and J. E. Crow, Phys. Rev. B **43**, 2989 (1991).
[16] I. Francois, C. Jaekel, G. Kyas, D. Dierickx, O. Van der Biest, R. M. Heeres, V. V. Moshchalkov, Y. Bruynseraede, H. G. Roskos, G. Borghs, and H. Kurz, Phys. Rev. B **53**, 12 502 (1996).
[17] D. H. Chen, S. R. Sheen, C. T. Chang, C. Y. Shei, and W-M. Hurng, J. Mater. Res. **7**, 2317 (1992).
[18] K. Kodama, S. Shamoto, H. Harashina, M. Sato, M. Nishi, and K. Kakurai, Physica C **263**, 333 (1996).
[19] N. Nagaosa and P. A. Lee, Phys. Rev. B **45**, 966 (1992).
[20] A. Matsuda, K. Kinishita, T. Ishii, H. Shibata, T. Watanabe, and T. Yamada, Phys. Rev. B **38**, 2910 (1988).
[21] Jeffery L. Tallon, Physica C **168**, 85 (1990).